The Interstellar Medium

Interstellar Gas

The diffuse matter between stars in our galaxy, commonly referred to as the "Interstellar Matter" (ISM), consists of gas, high-energy particles (Cosmic Rays), solid particles (dust) and radiation field. Magnetic fields permeate the interstellar gas, and the conductivity of the gas is large enough to consider the magnetic field to be frozen into the gas. Motion of the gas drags the magnetic field with it, conserving the magnetic flux through any blob of gas.

The energy density of the cosmic rays in the ISM is about 1 eV/cm^3, similar to the energy density of the diffuse interstellar radiation field. Interaction between a cosmic ray proton or heavy nucleus and the interstellar gas results in the heating of the gas, and also produces pions. The pions then decay into high-energy photons, producing gamma-rays. Most of the gamma-ray emission seen from the Galaxy originates in this process (fig. 1). This emission is seen as a thin strip in the sky, aligned with the so-called "Milky Way" seen in starlight. Since the gamma radiation produced by cosmic-ray interaction is a good tracer of the gas, this indicates that the gas in our galaxy is distributed not in an isotropic fashion, but is confined to a thin disk–a conclusion supported by observations of the gas by other means. The same is true of stars in our galaxy–which is the reason behind the appearance of the "Milky Way". Galaxies such as ours are called "disk galaxies". The thin disk-like structure is sustained due to angular momentum: large scale rotation of the gas and stars around the galactic centre. Often in these galaxies one finds spiral patterns of density enhancement, so they are also known as "spiral galaxies". The other major type of galaxies, called "elliptical galaxies", have a more three-dimensional distribution of stars and relatively little gas. Because of the lack of gas there is hardly any recent star formation in a typical elliptical galaxy, hence one mainly finds old (low-mass) stellar distribution in ellipticals, while the spirals are much more rich in young, massive stars.

Apart from the interaction with Cosmic Rays, the interstellar medium is heated in several other ways, for example ionisation by stellar radiation,

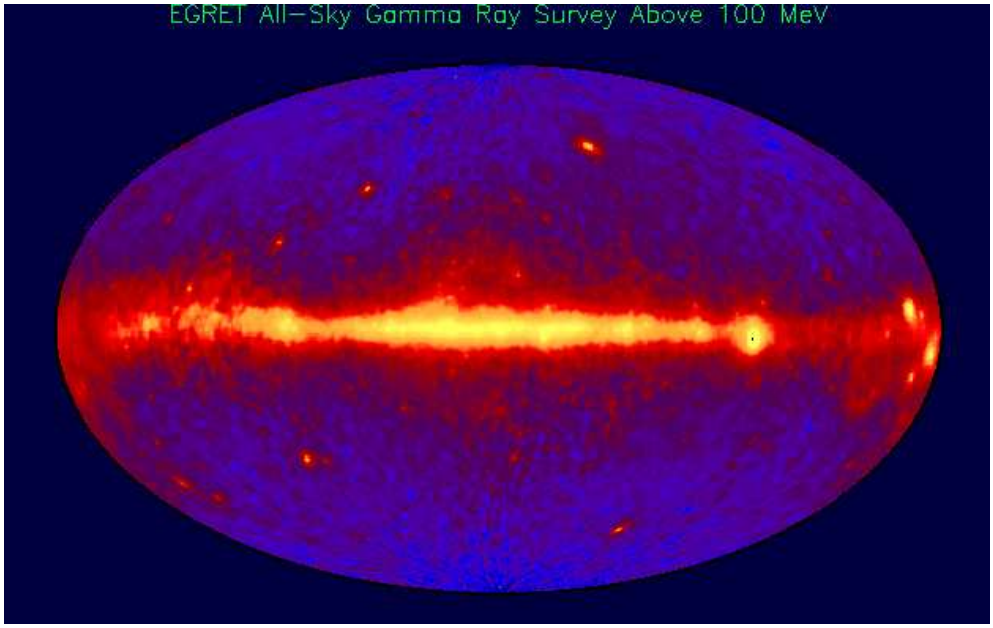

Figure 1: The all-sky gamma-ray map above 100 MeV obtained by the instrument EGRET (Energetic Gamma-Ray Experiment Telescope) on board the Compton Gamma Ray Observatory satellite. The figure is plotted in the Galactic coordinate system, where the plane of the milky way correspond to the central horizontal line and the Galactic centre is located at the centre of the figure. The diffuse gamma-ray emission produced by the interaction of Cosmic Rays with the gas in our galaxy is seen as the bright central band.

shock waves generated by supernovae and other violent phenomena, stellar winds and so on. Heated matter cools by radiation and expansion. Over sufficiently long time scales, the medium settles down to an overall equilibrium of heating and cooling. The resulting structure has several phases of the medium co-existing with each other in pressure equilibrium, at an average pressure $nT \sim 2000\text{cm}^{-3}\text{K}$. The major phases of the ISM are

- Coronal Gas: created mainly in the fast-expanding phase of supernova shocks. Temperature $T \gtrsim 10^6$ K.

- Warm Ionised Medium: $T \sim 8000$ K
- Warm Neutral Medium: $T \sim 6000$ K
- Cold Neutral Medium: $T \sim 80$ K
- Molecular Clouds: $T \lesssim 20$ K

In the densest molecular clouds self-gravity is important, and the central regions of them collapse to form stars. The envelope of the cloud is, however, prevented from collapsing into the core by the local magnetic field. As the cloud dimension shrinks, flux conservation leads to a rise in the magnetic field, and hence outward magnetic pressure, stabilizing the cloud.

The typical magnetic field strength in the interstellar space is a few microgauss, which implies an energy density similar to that in Cosmic Rays, as well as the interstellar gas pressure. Magnetic field is therefore important in controlling the dynamics of both these components. While the local magnetic field could stabilize a cloud against collapse, magnetic field also allows the thermal gas in the interstellar medium to drain downward along the magnetic field lines into the galactic potential well. The cosmic ray component would rise higher and be confined by the field. This creates regions where magnetic field buckles up from the galactic plane, and in the regions where they descend into the plane huge complexes of atomic and molecular gas clouds are formed.

The best probe of neutral atomic hydrogen in the Galaxy is the 21-cm hyperfine transition. From the study of this line, one has been able to map the density distribution of neutral gas in the Galaxy as well as study its dynamics. Neutral gas is distributed in a thin disk of width about 250 pc, while the radius of the Galaxy is $\sim$ 15 kpc. In the plane of the galaxy, the distribution of neutral hydrogen emission clearly shows the presence of a spiral structure. The spiral structure is even better defined in the distribution of bright HII regions, associated with massive stars.

The study of neutral Hydrogen and CO emission from molecular clouds has enabled us to determine the rotation of the gas in our galaxy. One finds

that gas and stars in the galactic disk rotate about the galactic centre, with the angular speed Ω a function of the galactocentric radius R. It turns out that the circular velocity ($v_c = R\Omega$) is nearly constant, at about 220 km/s, from $R \sim 2$ kpc outwards, much beyond the solar circle (orbit of the Sun, $R \sim 8$ kpc). The inferred mass included in an orbit of galactocentric radius R, given by $M(R) = Rv_c^2/G$, then continues to increase linearly with R well beyond most of the "visible" matter. This is a property shared by all disk galaxies. These galaxies presumably contain a large amount of matter that gives out almost no light. This is called the "missing mass" or the "dark matter" problem, and this non-luminous mass is assumed to lie in a dark halo. In our galaxy the luminous component adds up to about $10^{11} M_\odot$, while the dark halo contributes several times this amount.

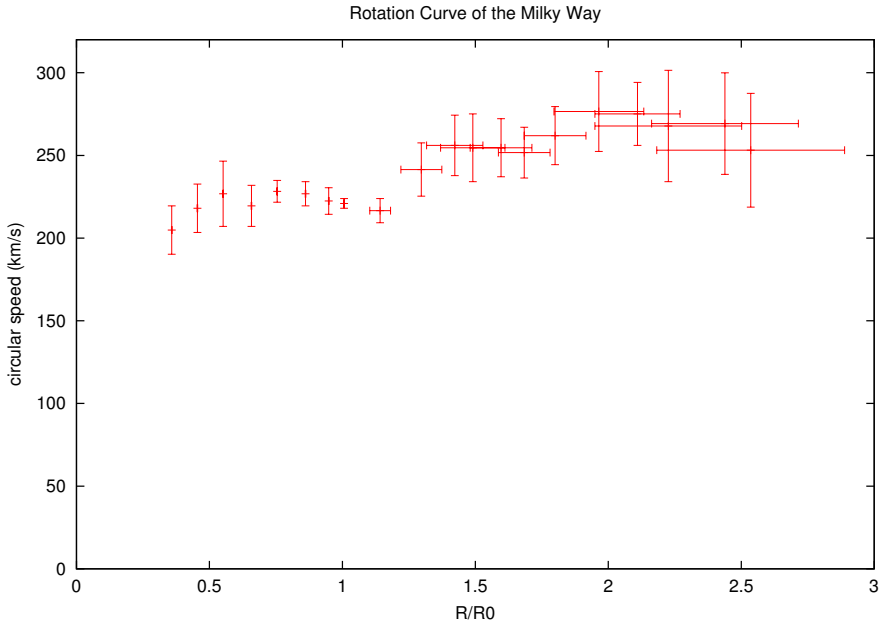

Figure 2: The Galactic rotation curve measured using the HI 21-cm and CO rotational lines (data from Honma and Sofue 1997 PASJ 49, 539). R_0 is the radius of the Solar Circle.

Free Electrons in the ISM

The degree of ionisation in the interstellar medium is non-zero nearly all over. Even well outside the so-called "ionised hydrogen regions", heavier elements like Carbon, with relatively loosely bound outer electrons, provide ionisation and hence a population of free, thermal electrons. This population is distinct from the ultrarelativistic non-thermal electrons responsible for the galactic synchrotron background. The average electron density in a typical line-of-sight through the Galaxy is $n_e \sim 0.03$ cm^{-3}: compare this with the average matter density, ~ 1 cm^{-3}.

These free electrons, and the corresponding background ions, form the interstellar plasma which makes its presence felt mainly through the propagation effects on radio frequency radiation through the ISM. We will discuss here two effects, Dispersion and Faraday Rotation.

The dispersion relation of electromagnetic waves in a plasma medium can be derived, starting from Maxwell's equations and explicitly including the effect of charges. In the absence of an electromagnetic distrubance, the net charge density in any volume is zero. The incident electromagnetic wave causes polarisation, inducing charge density oscillations. Let $\rho(\vec{r},t)$ be this charge density and $\vec{J}(\vec{r},t)$ the induced current density. The Maxwell's equations in Gaussian units then take the form

$$\begin{aligned}
\vec{\nabla}\cdot\vec{E} &= 4\pi\rho \\
\vec{\nabla}\cdot\vec{B} &= 0 \\
\vec{\nabla}\times\vec{E} &= -\frac{1}{c}\frac{\partial\vec{B}}{\partial t} \\
\vec{\nabla}\times\vec{B} &= \frac{4\pi}{c}\vec{J} + \frac{1}{c}\frac{\partial\vec{E}}{\partial t}
\end{aligned}$$

The oscillating quantities $\vec{E}$, $\vec{B}$, ρ and $\vec{J}$ can all be written as being proportional to $\exp\left[i(\vec{k}\cdot\vec{r}-\omega t)\right]$. On substitution, the Maxwell's equations yield

$$i\vec{k}\cdot\vec{E} = 4\pi\rho$$

$$\begin{aligned} i\vec{k}\cdot\vec{B} &= 0 \\ i\vec{k}\times\vec{E} &= i\frac{\omega}{c}\vec{B} \\ i\vec{k}\times\vec{B} &= \frac{4\pi}{c}\vec{J} - i\frac{\omega}{c}\vec{E} \end{aligned}$$

We now need to find the relation between ρ, $\vec{J}$ and $\vec{E}$, $\vec{B}$. Because ions are much heavier than the electrons, we assume that only the electrons move under the influence of the incident field and the ions form a fixed background. We also assume that all motions are non-relativistic. Since $v \ll c$, the magnetic term in the Lorentz force can be neglected (as, for the electromagnetic wave, $|\vec{E}| = |\vec{B}|$). The motion of the electrons are then described by

$$m_e\dot{\vec{v}} = -e\vec{E} \text{ i.e. } -im_e\omega\vec{v} = -e\vec{E}$$

Hence

$$\vec{v} = \frac{e\vec{E}}{i\omega m_e} \text{ and } \vec{J} = -n_e\vec{v}e = \frac{in_e e^2}{\omega m_e}\vec{E}$$

So $\vec{J}$ can be written as $\sigma\vec{E}$ with conductivity

$$\sigma = \frac{in_e e^2}{\omega m_e}$$

We can now determine ρ in terms of $\vec{E}$ using the charge continuity equation:

$$\begin{aligned} \frac{\partial\rho}{\partial t} + \vec{\nabla}\cdot\vec{J} &= 0 \\ \text{hence } -i\omega\rho + i\vec{k}\cdot\vec{J} &= 0 \end{aligned}$$

Which yields

$$\rho = \frac{\vec{k}\cdot\vec{J}}{\omega} = \frac{\sigma}{\omega}\vec{k}\cdot\vec{E}$$

Substituting the above expressions for ρ and $\vec{J}$ in the Maxwell's equations one obtains

$$\begin{aligned} i\vec{k}\cdot(\epsilon\vec{E}) &= 4\pi\rho \\ i\vec{k}\cdot\vec{B} &= 0 \end{aligned}$$

$$\begin{aligned} i\vec{k}\times\vec{E} &= i\frac{\omega}{c}\vec{B} \\ i\vec{k}\times\vec{B} &= -i\frac{\omega}{c}(\epsilon\vec{E}) \end{aligned}$$

Where

$$\epsilon = 1 - \frac{4\pi\sigma}{i\omega} = 1 - \frac{4\pi n_e e^2}{m_e\omega^2} = 1 - \frac{\omega_p^2}{\omega^2}$$

acts as the dielectric constant of the plasma medium. The quantity

$$\omega_p = \sqrt{\frac{4\pi n_e e^2}{m_e}} \approx 2\pi\times 10^4 \sqrt{\frac{n_e}{1\ \mathrm{cm}^{-3}}}\ \mathrm{Hz}$$

is defined as the "plasma frequency" of the medium. This gives a dispersion relation

$$\begin{aligned} c^2k^2 &= \epsilon\omega^2 \\ \text{or } k &= \frac{\omega}{c}\left(1 - \frac{\omega_p^2}{\omega^2}\right)^{1/2} \end{aligned}$$

This shows that the medium inhibits propagation for $\omega < \omega_p$, and that the medium is dispersive at $\omega > \omega_p$. The phase velocity of the wave is

$$\mathrm{v_p} = \frac{\omega}{k} = \frac{c}{\sqrt{1-\omega_p^2/\omega^2}}$$

which is larger than c. The group velocity, however, is

$$\mathrm{v_g} = \frac{d\omega}{dk} = c\sqrt{1-\omega_p^2/\omega^2}$$

smaller than c. The propagation speed of a signal is larger at higher frequencies, and approaches c at $\omega \gg \omega_p$.

The most used practical application of this is in the study of radio pulsars. The lower the observing frequency, the later the pulses arrive at the observer, the arrival time being given by

$$t_a = \int_0^L \frac{ds}{v_g(\omega)}$$

The rate of change of arrival time with observing frequency can be measured and the total dispersion along the line of sight deduced. If L is the distance to the pulsar then

$$\begin{aligned}
\frac{dt_a}{d\omega} &= \int_0^L \frac{ds}{c}\left[\frac{d}{d\omega}\left(\frac{1}{\sqrt{1-\omega_p^2/\omega^2}}\right)\right] \\
&= \int_0^L \frac{ds}{c}\left[\frac{d}{d\omega}\left(1+\frac{\omega_p^2}{2\omega^2}\right)\right] \\
&= -\int_0^L \frac{ds}{c}\frac{\omega_p^2}{\omega^3} \\
&= -\frac{4\pi e^2}{m_e c\omega^3}\int_0^L n_e ds \\
&= -\frac{4\pi e^2}{m_e c\omega^3}\mathrm{DM}
\end{aligned}$$

where we have assumed $\omega^2 \gg \omega_p^2$ and defined the "Dispersion Measure" DM$\equiv \int_0^L n_e ds$. Measurement of DM can help determine the average electron density in the line of sight if the distance to the pulsar is known (via, say, parallax or the relative motion between the Sun and the ISM in the vicinity of the pulsar due to galactic differential rotation, determined using the HI absorption line). On the other hand if the average line-of-sight electron density is known, one can use DM to estimate distances to pulsars.

In the presence of a local Magnetic Field, the above Dispersion relation is modified further. The motion of an electron is now influence, in addition to the oscillatory electric field, also by the ambient magnetic field $\vec{B}_0$:

$$m_e\dot{\vec{\mathrm{v}}} = -e\vec{E} - \frac{e}{c}\vec{\mathrm{v}}\times\vec{B}_0$$

Electrons would gyrate in the local magnetic field, with frequency $\omega_c = eB_0/m_e c$. The eigenmodes of the propagating electromagnetic field in such a medium are circularly polarised:

$$\vec{E}(t) = E_1(\hat{\epsilon_1} \mp i\hat{\epsilon_2})\exp(-i\omega t)$$

being a typical representation of the modes at a given point in space. $\hat{\epsilon_1}$ and $\hat{\epsilon_2}$ are two orthogonal unit vectors, in a plane normal to the direction of propagation. The upper sign corresponds to a right circular polarisation and the lower one to a left circular polarisation. For the sake of simplicity, we assume that the propagation is along the local magnetic field $\vec{B} = B_0\hat{\epsilon_3}$. The force equation then yields:

$$\vec{v} = \frac{e\vec{E}}{im_e\omega(1 \pm \omega_c/\omega)}$$

This leads to

$$\sigma = \frac{in_e e^2}{m_e\omega(1 \pm \omega_c/\omega)}$$

and

$$\epsilon = 1 - \frac{4\pi\sigma}{i\omega} = 1 - \frac{\omega_p^2}{\omega^2(1 \pm \omega_c/\omega)}$$

The dispersion relation for the circularly polarised modes are then

$$\begin{aligned} k &= \frac{\omega}{c}\sqrt{\epsilon} \\ &= \frac{\omega}{c}\left[1 - \frac{1}{2}\frac{\omega_p^2}{\omega^2}\left(1 \mp \frac{\omega_c}{\omega}\right)\right] \quad (\omega \gg \omega_p,\omega_c) \end{aligned}$$

After propagation through a distance L in the medium, the angle of phase rotation of each of the circularly polarised modes is

$$\phi_{\mathrm{R,L}} = \int_0^L k_{\mathrm{R,L}} ds$$

If the incident polarisation is linear, this amounts to a net rotation of the plane of polarisation by

$$\theta = \frac{1}{2}(\phi_{\mathrm{R}} - \phi_{\mathrm{L}}) = \frac{1}{2}\int_0^L (k_{\mathrm{R}} - k_{\mathrm{L}}) ds$$

Using the dispersion relation, this becomes

$$\begin{aligned} \theta &= \frac{1}{2c}\int_0^L ds \frac{\omega_p^2\omega_c}{\omega^2} \\ &= \left[\frac{e^3}{2\pi m_e^2 c^4}\int_0^L n_e B_0 ds\right]\lambda^2 \end{aligned}$$

This is called the "Faraday Rotation". The rotation suffered by the plane of polarisation is proportional to the square of the wavelength λ, with a coefficient, given by the quantity in square brackets in the above equation, called the "Rotation Measure". The Rotation Measure is directly proportional to the integral of the line-of-sight component of the magnetic field, weighted by electron-density. The measurement of both the Rotation Measure and the Dispersion Measure of a pulsar then yields an estimate of the interstellar magnetic field. In practice this gives an upper limit to the line-of-sight component of the magnetic field since the field could undergo direction reversals in the intervening medium.

Dust

The interstellar medium, in addition to gas and free electrons, also contains solid particles (grains) of size comparable to the wavelength of visible light. Collectively, these solid particles are referred to as *Dust*.

The dust grains are made up of metal silicates and oxides, graphite, silicon carbide and other such stable, heat-resistant (refractory) compounds into which elements available in the interstellar matter can condense. Indeed the constituent elements of dust grains are found to be *depleted* in interstellar clouds, with the amount of depletion directly correlated with the condensation temperature of the element.

The interstellar dust makes its presence felt with strong *extinction* at optical wavelengths. Extinction is the removal of light from the direction of propagation due to the combined effect of scattering and absorption. The *extinction efficiency* Q_e measures the "optical cross section" (which is the sum of scattering and absorption cross sections) of the grain in units of its geometrical cross section πa^2, where a is the radius of the grain.

$$Q_e = Q_s + Q_a$$

where Q_s and Q_a are scattering and absortion cross sections respectively. The ratio Q_s/Q_e is the *albedo* of the grain.

With the source of light being a hot star or a stellar complex, the dust grains in the surrounding medium produce a diffuse, extended glow of scattered

light. Such a glow is known as a "reflection nebula". A clear example of this is found near the hot stars in the spectacular Orion Nebula (fig. 3).

Figure 3: Reflection nebula near the "belt of three stars" in Orion

The fraction of incident radiation that is absorbed by a dust grain raises its temperature, and is re-radiated, primarily in the Infrared.

For an incident wavelength λ, if we define a quantity $x = 2\pi a/\lambda$, then Q_s and Q_a can be expressed as functions of x, and of the refractive index μ. In general μ is complex, with the imaginary part giving rise to absorption. Theoretical computation of the extinction efficiency can be carried out using the Mie theory of scattering. We will not discuss the details here, but illustrate some results.

At $\mu x \ll 1$, i.e. $\lambda \gg a$ one is in the regime of Rayleigh scattering, and the scattering efficiency goes as x^4. At $\mu x \gg 1$, i.e. $\lambda \ll a$, the total extinction efficiency Q_e settles down to 2. The reason for this is as follows. According to Babinet's principle the diffraction pattern due to a circular obstacle is identical to that due to a circular aperture of the same size. So clearly a circular obstacle removes from the incoming beam, in addition to the energy striking the obstacle directly, an equal amount of energy by diffraction. In the intermediate regime, interference effects cause Q_e, Q_s to oscillate, with a broad maximum reached in the range $x \sim$ a few depending on the refractive index. An example is shown in figure 4.

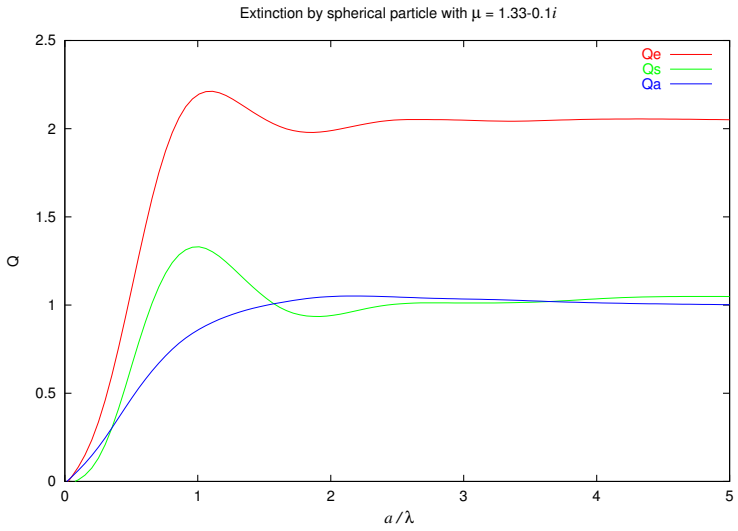

Figure 4: The extinction cross section Q_e (red), scattering cross section Q_s (green) and absorption cross section Q_a (blue) in units of the geometrical cross section of a spherical grain of refractive index $\mu = 1.33 - 0.1i$, plotted against a/λ, where a is the radius of the grain and λ is the wavelength of the incident light

The amount of extinction caused by dust in the line of sight to a source can be determined if the intrinsic spectral characteristics of the source are known; one can use standard stars for this purpose. The amount of extinction thus determined is normally expressed in terms of an excess magnitude A_λ at an wavelength λ, i.e. the observed magnitude at that wavelength is

$$m = m_0 + A_\lambda$$

where m_0 would be the apparent magnitude in absence of dust extinction.

The average extinction law in the Galaxy, normalised to the extinction in V band, is shown in figure 5, and the relative values of A_λ in some standard photometric bands are listed in Table 1. It is not possible to explain the observed wavelength dependence in terms of a single species of grain. The bump near the wavelength of 0.22 micron is thought to be due to graphite

Table 1: Galactic extinction of some standard photometric bands. $\lambda_{\rm eff}$ is the effective wavelength in microns. The last column quotes the extinction in units of the extinction at V band, for average Galactic extinction law ($R_V = 3.1$)

System	Band	$\lambda_{\rm eff}$ (μ)	A/A_V
Johnson	U	0.3652	1.56
	B	0.4448	1.32
	V	0.5505	1.00
	R	0.6930	0.76
	I	0.8785	0.50
Cousins	$R_{\rm C}$	0.6588	0.81
	$I_{\rm C}$	0.8060	0.59
Infrared	J	1.22	0.29
	H	1.63	0.18
	K	2.19	0.11
	L	3.45	0.05
	M	4.75	0.03

particles, although recently a case is being made in favour of Polycyclic Aromatic Hydrocarbons (PAHs). At least two more dominant species of grains are required to explain the general nature of the extinction: most probably Magnesium and Aluminium Silicates for the ultraviolet region and possibly Silicon Carbide for the Infrared region. Over the years, it has been realized that many different materials with a wide variety of optical properties can be used to explain the extinction curve, suggesting that it is relatively insensitive to the exact dust composition.

The nature of the extinction curve shows that with the exception of the UV hump, the extinction is larger at shorter wavelengths. This means that extinction not only affects the apparent total intensity of the source but also its colour. This effect is called *reddening*. The amount of reddening is

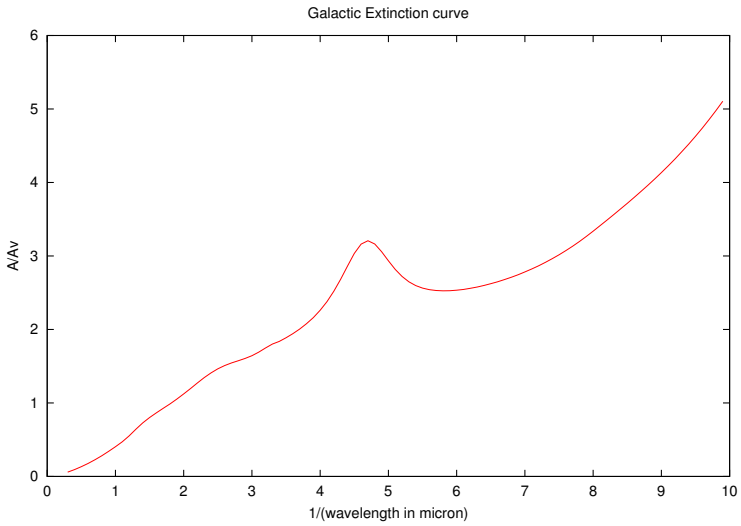

Figure 5: Wavelength dependence of average interstellar extinction in our Galaxy.

usually expressed as the "colour excess"

$$E(B-V) = (B-V) - (B_0 - V_0) = A_B - A_V = \left(\frac{A_B}{A_V} - 1\right) A_V = \frac{A_V}{R_V}$$

where B and V are the measured apparent magnitudes in the B and V photometric bands, and those with suffix 0 are what they would have been in absence of extinction. A_B and A_V are the extinction at the effective wavelengths of B and V bands. The last equality above defines R_V, the value of which for the average Galactic extinction law shown in fig. 5 works out to 3.1.

If the grain is not spherical, then its extinction efficiency becomes anisotropic. The electric vector parallel to the long axis is extinguished more than that perpendicular to it. So for an unpolarized incident radiation, the emergent light becomes partially linearly polarized, with the position angle perpendicular to the long axis of the grain. In the interstellar space, polarization up to several percent can arise in this manner.

Dust grains also undergo collisions with the gas particles in the vicinity,

which sets them rotating and also builds up static electric charges on them. This results in a magnetic moment:

$$M = \frac{Z_d e \langle z^2 \rangle \omega}{2c}$$

where $Z_d e$ is the charge on the dust grain, ω its rotation speed and $\langle z^2 \rangle$ the mean square displacement of the charge from the rotation axis. On an average, the largest component of M would be perpendicular to the long axis of the grain, as $\langle z^2 \rangle$ is maximum for this.

In the presence of an external magnetic field $\vec{B}$, the grain will then precess, so as to keep the average orientation of its long axis perpendicular to $\vec{B}$. Grains act as paramagnetic substances with a complex susceptibility, and the oscillating magnetisation set up by the precession is damped by draining energy away from rotation. This drags the grain magnetic moment closer to $\vec{B}$, resulting in an average alignment of the grains with long axis perpendicular to $\vec{B}$. Starlight passing through a collection of these grains will then exhibit preferential polarization parallel to the local magnetic field $\vec{B}$. Observations of the polarization of starlight have thus helped in mapping the distribution of the magnetic field in the Galaxy.

The equilibrium temperature of a dust grain is decided by the balance between heating by absorbed starlight and cooling by radiation. The process is similar to the establishment of the equilibrium temperature of the Earth by the absorption of Solar energy. If the incident radiation on a dust grain can be expressed as a "diluted black body radiation" at a temperatute T_* and dilution factor W (if the source of radiation is a single star then W is just the solid angle subtended by the star at the location of the dust grain), and if T_g is the temperature of the grain, then if Q_a is nearly unity near both $\lambda_* = hc/kT_*$ and $\lambda_g = hc/kT_g$ then

$$T_g \approx W^{1/4} T_*$$

However, in general we need to take into account the wavelength dependence of Q_a, and the emitted radiation from the grain equals

$$L_g(T_g) = 4\pi \int_0^\infty Q_a(\lambda) B_\lambda(T_g) d\lambda$$

and the resulting dust temperature has the form

$$T_g \approx W^{1/5} T_*$$

The diffuse interstellar radiation field can be approximated by a T_* of $\sim 10^4$ K and $W \sim 10^{-14}$, giving a typical interstellar grain temperature of ~ 15 K. The dust in HII regions are heated to about twice this temperature, and grains near O stars attain temperatures of $\sim 100\ K$. The emitted radiation from the grains are therefore mainly in infrared, and copious infrared luminosity can be emitted if there is an abundance of young, high-mass stars in relatively dense regions where dust can exist. Infrared radiation is thus an excellent tracer of star forming regions. Space-based infrared observatories such as ISO have discovered a whole population of galaxies which are extremely bright in infrared, called ULIRGs (Ultra Luminous Infrared Galaxies). These are thought to be galaxies where very strong recent star formation has occurred. They are also referred to as *starburst* galaxies. In general, the Far Infrared (FIR) luminosity gives a good measure of the current star formation activity in any galaxy. Dust in external galaxies is also vividly represented in the prominent, dark "dust lanes" visible in their optical images (see fig. 6).

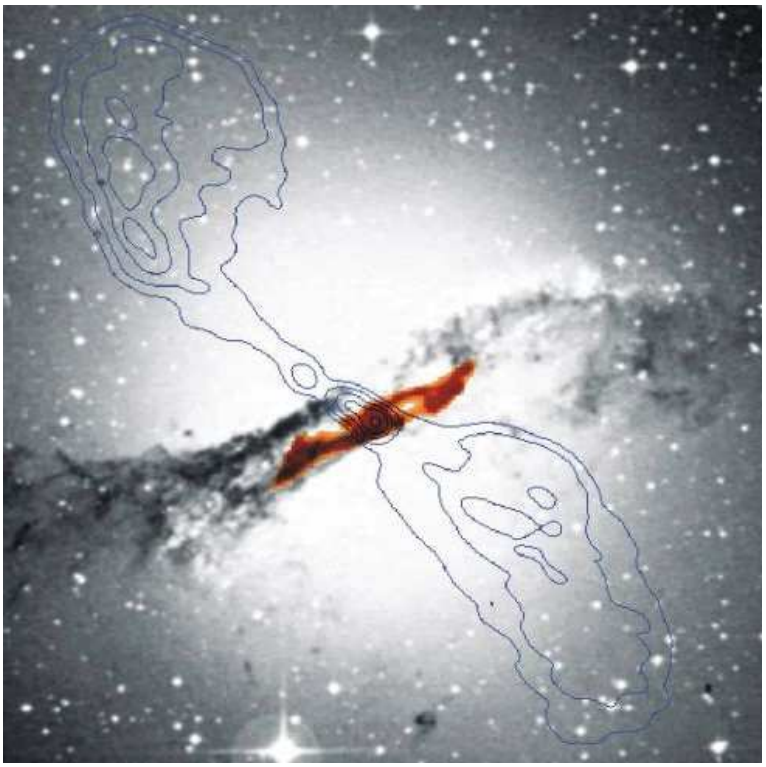

Figure 6: A composite image of the nearest active galaxy Centaurus A. white shows optical emission, red the infrared emission mapped by the ISO satellite and the contours trace the lobes of radio emission. The wide dark band across the middle of the galaxy is a prominent Dust Lane. This galaxy is a Giant Elliptical (as seen in the optical light), that harbors another barred spiral galaxy inside (as revealed in the thermal emission from dust imaged by ISO). The bar of the embedded spiral helps feed a massive black hole at the centre, which is responsible for AGN activity, including the radio emission